Available online at www.sciencedirect.com
SCIENCE DIRECT
Journal of Colloid and Interface Science 297 (2006) 525–533
JOURNAL OF Colloid and Interface Science
www.elsevier.com/locate/jcis

Investigation on γ-cyclodextrin nanotube induced by N,N'-diphenylbenzidine molecule

Aihua Wu, Xinghai Shen *, Yongke He

Department of Applied Chemistry, College of Chemistry and Molecular Engineering, Peking University, Beijing 100871, People's Republic of China

Received 16 July 2005; accepted 7 November 2005

Available online 13 December 2005

Abstract

Dynamic light scattering (DLS) measurement provides an effective way to investigate the formation of nanotube of γ-cyclodextrin (γ-CD) induced by N,N'-diphenylbenzidine (DPB) in water. With the combination of steady-state fluorescence and fluorescence anisotropy experiments, it was found that for α- and β-CD, only 1:2 (guest:host) inclusion complexes were formed and for γ-CD, cyclodextrin nanotube was formed involving 16 γ-CD units at maximum. The pH effect studies with both DLS and fluorescence anisotropy measurements indicated that the hydrogen bonding between neighboring CDs was necessary to the formation of cyclodextrin nanotube. In the temperature experiment, we found that the nanotube of DPB-γ-CD could exist stably at relatively high temperatures and the transition point for structural collapse was estimated to be around 54 °C. The aggregation states of both γ-CD itself and DPB-γ-CD nanotube were observed with TEM.

Keywords: Dynamic light scattering; Cyclodextrin nanotube; Fluorescence anisotropy; Hydrogen bonding; TEM

1. Introduction

Cyclodextrin (CD), containing 6 (α-CD), 7 (β-CD), or 8 (γ-CD) D-glucose units, is one of the most popular host molecules to construct various molecular assemblies. It is well known that cyclodextrin and its derivatives can selectively incorporate guest molecules through size matching and weak interactions, such as hydrophobic interaction, van der Waals' force and hydrogen bonding [1,2]. Depending on its size, a CD molecule has room to accommodate one or two guest molecules in most cases; if the guest is long enough, three [3] or even many CD rings [4] can be threaded along it. A series of nanotubes have been chemically synthesized by Harada et al. using α-CD and polymers [5,6]. Li and his co-workers found that nanotubes of β- and γ-CD incorporated with a rod-like molecule, i.e., all-trans-1,6-diphenyl-1,3,5-hexatriene (DPH) could be formed just through supramolecular assembly [7]. Later, Pistolis et al. corroborated the results by a detailed study on the size effect of the homologues of the α,ω-diphenylpolyebes series, with two, three and four double bonds, on the formation of nanotubes with γ-CD [8,9]. Agbaria and Gill discovered that some oxazole molecules could also lead to the formation of nanotubes of γ-CD in aqueous solutions [10–12]. Liu et al. have focused on the artificial design of nanotubes induced by cyclodextrin derivatives and metal ions through the metal ion-ligand coordination [13–15]. In addition, nanotubular structure can also be formed between some drug molecule and surfactant with cyclodextrin [16]. Besides the above examples through bimolecular interactions, one-dimensional self-assembly of some cyclodextrin derivatives themselves also formed nanotubular structures in the solid state [17,18]. Our research group is also interested in the studies concerning the formation of cyclodextrin nanotubes induced by organic molecules and aims to find out what kinds of organic molecules can benefit the formation of cyclodextrin nanotube. So far, several molecules, such as 2-phenyl-5-(4-diphenylyl) 1,3,4-oxadiazole (PBD), butyl-PBD, 2,2′-biquinoline (BQ), 1,1′-(methylenedi-1,4-phenylene) bismaleimide (MDP-BMI), and 4,4′-bis(2-benzoxazolyl) stilbene (BOS) have been studied [19–23].

* Corresponding author. Fax: +86 10 62759191.
E-mail address: xshen@pku.edu.cn (X. Shen).

0021-9797/$ – see front matter
doi:10.1016/j.jcis.2005.11.014

Nowadays, NMR, X-ray diffraction, transmission electron microscopy and steady-state fluorescence anisotropy have become the common methods of characterizing cyclodextrin nanotubes. Dynamic light scattering (DLS) permits an estimation of the diffusion coefficient from which the hydrodynamic radius of particle (R_h) can be estimated using the Stokes–Einstein equation for a spherical particle [24]. As a general method of determining particle size, this technique has been proven to be advantageous in the study of macromolecular systems and supramolecular assemblies [25]. However, to the best of our knowledge, DLS is seldom used to study cyclodextrin nanotubes, especially those induced by small molecules. Gonzalez-Gaitano and Brown studied the interactions between dimethylated β-CD and nonionic polymeric surfactants with combination of static and dynamic light scattering and found that approximately 11 dimethylated β-CD molecules were threaded onto a copolymer chain to form a tubular structure of cyclodextrin [26]. In order to apply the DLS technique to the investigation on cyclodextrin nanotubes, it is necessary to ascertain the self-aggregation phenomenon of cyclodextrin itself. Actually, the existing state of cyclodextrin in pure water still remains controvertible to some extent [27,28]. Recently, the self-aggregation of cyclodextrins and inclusion complexes between cyclodextrins and guest molecules has been investigated through DLS [29–32]. Coleman et al. [29] observed the aggregates of CDs and then Gonzalez-Gaitano et al. [31] carefully studied the ability of self-aggregation of CDs in aqueous solution and found that they could form large and polydisperse aggregates in spite of their much smaller contribution in mass than that of monomeric CDs.

In this article, we apply DLS technique to investigate the formation of a cyclodextrin nanotube induced by DPB (see Scheme 1). Since the formation of nanotube is dependent on CD concentrations, static light scattering is not suitable to be used in this system. To demonstrate the validity of DLS results, we have also carried out the measurements of steady-state fluorescence and fluorescence anisotropy on DPB-α-CD, DPB-β-CD, and DPB-γ-CD systems. Furthermore, TEM images show directly the large particles aggregated by γ-CD molecules. And the nanotubular structure in the DPB-γ-CD system can also be observed.

DPB and its derivatives belong to a class of light emitting and charge transporting materials that are used in displays, photovoltaic cells, and electrophotographic photoreceptors [33–35]. Hence, we think the cyclodextrin nanotube formed between DPB and γ-CD, in which the DPB molecule is restrained and arrayed linearly in the γ-CD cavity, may have some potential applications as mentioned.

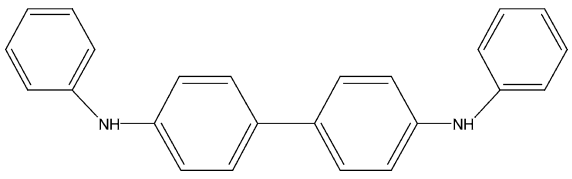

Scheme 1. Molecular structure of DPB.

2. Materials and methods

2.1. Materials

DPB (Acros, 99%), α-CD (Acros, >98%), and γ-CD (Acros, 99%) were used as received. β-CD (Beijing Shuanghuan, China) was recrystallized three times from tridistilled water. All other chemical reagents used in this study were of analytical grade.

2.2. Instruments

DLS measurements were performed on an ALV/DLS/SLS-5022F photon correlation spectrometer. The wavelength of laser was 632.8 nm, and the scattering angle was 90°. The size distribution was obtained from the intensity autocorrelation functions that were analyzed using the methods of Contin [36]. The temperature was controlled at 25 °C. The experimental error of DLS measurement is about 5%.

The viscosity was measured by Ubbelohde viscometer at 25 °C.

Absorption spectra were recorded on an U-3010 (Hitachi) spectrophotometer, and the slit width was 2 nm. Steady-state fluorescence and anisotropy measurements were performed on a F-4500 (Hitachi) spectrofluorimeter. Both the excitation and emission slit widths were 10 nm. Each solution was excited near its maximum absorption wavelength using 1 cm quartz cells. The pH values were adjusted by adding NaOH, no buffers were used for all the solutions investigated. In the experiment, the temperature control was achieved with the sample placed in a cell compartment whose walls were accessible to water circulation. Water from a thermostated bath was allowed to circulate through the walls of the sample compartment. The final temperature of the sample was measured by means of a thermocouple (Checktemp, Hanna, Italy) (±0.1 °C) immersed in the solution.

Fluorescence lifetime measurements were made on a multiplexed time-correlated single-photon counting fluorimeter FLS920 (EDINBURGH). The fluorescence lifetime was determined from data on the fluorescence transient waveform of the material to be tested and the lamp waveform data using the least-squares iterative deconvolution method. The maximum absorption wavelengths for DPB molecule in pure water, α-, β-, and γ-CD were 336, 336, 341, and 343 nm, respectively. The maximum emission wavelengths were 410, 410, 385, and 385 nm, respectively. 3000 counts were collected for each sample.

Micrographs of transmission electron microscopy (TEM) were obtained with a JEM-100CX II, high-resolution TEM (H-9000, Hitachi) by the negative staining method. Uranyl acetate solution (2%) was used as the staining agent. One drop of the sample solution was placed onto a formvar-coated copper grid.

2.3. Methods

Stock solution of DPB was prepared in methanol. Tridistilled water and fresh sample solutions were used throughout the experiments.

Dynamic light scattering measurement is based on the autocorrelation function of the intensity signal. The convolution of the intensity signal as a function of time contains information about the dynamic properties of the solute molecules. The most direct information obtained is the translational diffusion coefficient which, for a spherical molecule, is related to the radius, R_h, according to the Stokes–Einstein relationship [24],

$$R_h = k_B T/6\pi\eta_0 D_0, \quad (1)$$

where k_B is the Boltzmann constant, T the temperature, η_0 the solvent viscosity, and D_0 the diffusion coefficient at infinite dilution. Samples were filtered prior to the measurements with 0.2-μm filter (Membrana, micro PES) or 0.02-μm filter (Whatman, inorganic membrane).

Steady-state fluorescence anisotropy was used to determine the rotation degree of DPB/CDs complexes. The anisotropy r, measured by front-face excitation [37], can be given by

$$r = (I_{VV} - GI_{VH})/(I_{VV} + 2GI_{VH}), \quad (2)$$

where I_{VV} is the intensity with vertical orientations of both excitation and emission polarizers, while I_{VH} with vertical and horizontal orientations, respectively. The G factor, an instrumental factor reflecting the polarization characteristics of the photometric system, is defined as

$$G = I_{HV}/I_{HH}, \quad (3)$$

where I_{HH} is the intensity with horizontal orientations of both excitation and emission polarizers, while I_{HV} with horizontal and vertical orientations, respectively.

3. Results and discussion

3.1. DLS analysis

Fig. 1 shows the DLS results of size distributions in the aqueous solutions of CDs in the absence and presence of DPB molecule, respectively, which are also summarized in Table 1. In the absence of DPB molecule, the aqueous solutions of CDs exhibit two kinds of size, one with mean hydrodynamic radius less than 1 nm and the other larger than 60 nm. We assign the small size to the monomeric CD and the large size to the self-aggregated CD on the basis of the results reported by Gonzalez-Gaitano et al. [31]. It should be pointed out here that we observed bimodal distribution for α-, β-, and γ-CDs when the samples were treated with 0.2-μm filter, while Gonzalez-Gaitano et al. just observed aggregated forms of β- and γ-CD with 0.2-μm filter and the monomeric form was detected with 0.1-μm filter. For α-CD, however, both monomeric and aggregated forms were detected even with 0.2-μm filter [31]. We also note that Coleman et al. did not report the detection of monomeric CD [29].

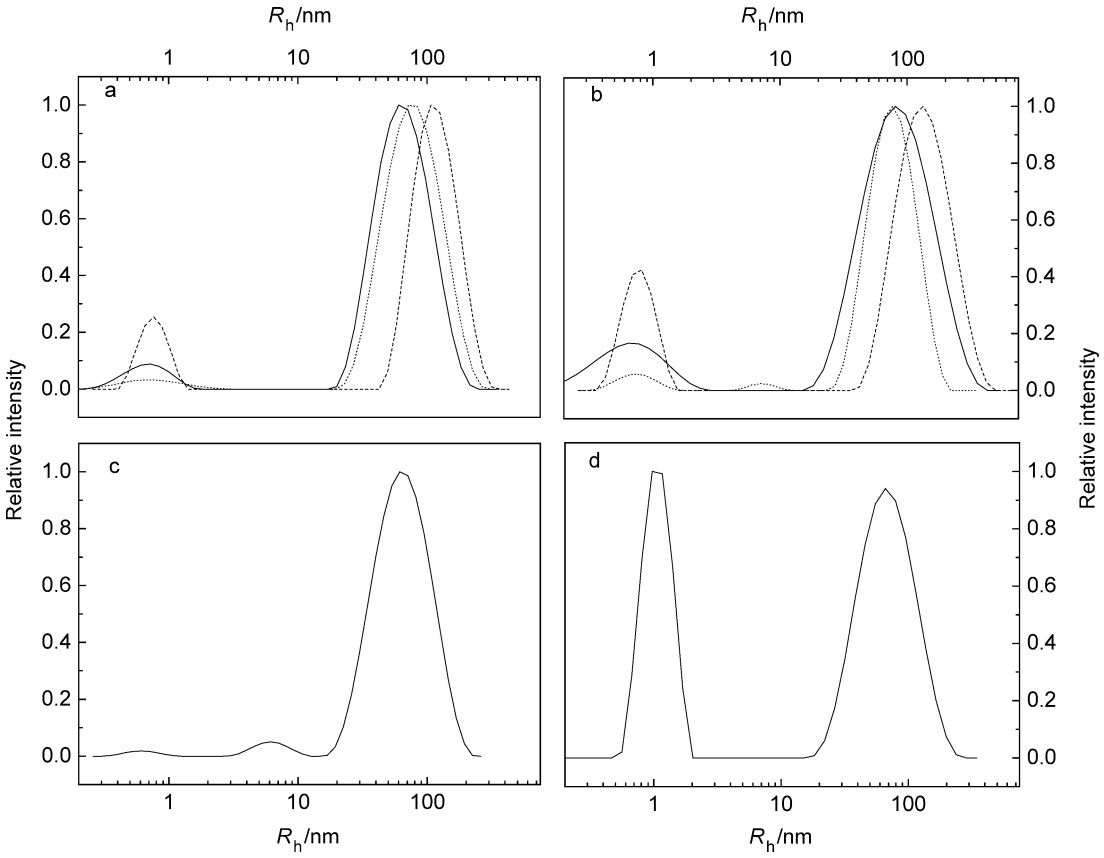

Fig. 1. (a) DLS results of the aqueous solutions of α-CD (solid line), β-CD (dash line), and γ-CD (dot line) treated with 0.2-μm filter; (b) DLS results of the aqueous solutions of α-CD (solid line), β-CD (dash line), and γ-CD (dot line) in the presence of DPB treated with 0.2-μm filter; (c) DLS result of the aqueous solution of DPB-γ-CD treated with 0.02-μm filter; (d) DLS result of the aqueous solution of DPB-γ-CD at pH 13.5 treated with 0.2-μm filter. [DPB] $= 4 \times 10^{-7}$ M, [CD] = 10 mM.

Table 1
Mean hydrodynamic radius (R_h), correlative intensity (I), and mass (M) contributions of various components in the aqueous solutions of CDs and DPB-CDs filtered with 0.2- and 0.02-μm* filters. [DPB] = 4×10^{-7} M, [CD] = 10 mM

Sample	R_{h1} (nm)	I_1 (%)	M_1 (%)	R_{h2} (nm)	I_2 (%)	M_2 (%)	R_{h3} (nm)	I_3 (%)	M_3 (%)
α-CD	0.6 ± 0.1	6.68	99.9989	–	–	–	64.4 ± 0.5	93.32	0.0011
DPB-α-CD	0.6 ± 0.1	13.98	99.9998	–	–	–	82.2 ± 0.6	86.02	0.0002
β-CD	0.8 ± 0.1	14.02	99.9998	–	–	–	114.7 ± 0.4	85.98	0.0002
DPB-β-CD	0.8 ± 0.1	20.61	99.9999	–	–	–	133.3 ± 0.5	79.39	0.0001
γ-CD	0.7 ± 0.2	3.19	99.9977	–	–	–	76.7 ± 0.5	96.81	0.0023
DPB-γ-CD	0.7 ± 0.1	4.25	99.9729	7.2 ± 0.2	1.17	0.0253	75.3 ± 0.4	94.58	0.0018
DPB-γ-CD*	0.7 ± 0.2	0.97	99.6660	6.8 ± 0.3	2.86	0.3206	63.1 ± 0.5	96.17	0.0134
DPB-γ-CD (pH 13.5)	1.1 ± 0.1	39.85	99.9993	–	–	–	67.1 ± 0.5	60.15	0.0007

It seems that the experimental conditions affect remarkably the detected results.

It can be seen from Fig. 1 and Table 1 that the size distributions of α- and β-CD in the presence and absence of DPB are very similar. In other words, the presence of DPB and the possible formation of inclusion complexes do not influence obviously the DLS results on CD forms. But interestingly, one can find a new peak with mean hydrodynamic radius at about 7 nm in the aqueous solution of γ-CD in the presence of DPB. It is believed that this corresponds to a new structure other than monomeric and aggregated γ-CD. Based on our previous work [19–23], we think that this new peak is caused by the formation of cyclodextrin nanotube. Similarly, a novel DLS peak around 17 nm was ascribed to the formation of micelle in the mixed system of cationic bolaamphiphile BPHTAB (biphenyl-4,4′-bis(oxyhexamethylenetrimethylammonium bromide)) and its oppositely charged conventional surfactants [36]. In the cases of α- and β-CD with DPB added, only 1:1 (guest:host) and/or 1:2 inclusion complexes, but not nanotube, could be formed. The sizes of simple inclusion complexes detected by DLS might have minute difference with that of monomeric CD, as shown in Fig. 1. The approximate calculation of mass contributions of all components has been carried out using the method suggested by Gonzalez-Gaitano et al. for spherical model [31] (see Table 1). Although the intensity contribution for the aggregated CD is dominating, its mass contribution is very low, i.e., 0.0011, 0.0002, and 0.0023% for α-, β-, and γ-CDs, respectively. The calculation result for α-CD is in good agreement with that in Ref. [31]. These results strongly suggest that the monomeric forms of α-, β- and γ-CDs are predominated in their aqueous solutions. The calculated mass contribution of nanotube in the DPB-γ-CD system is 0.0253%. Thus, the occurrence of the new DLS peak is a good indication of the formation of cyclodextrin nanotube. To further ascertain the appearance of the new peak in the DPB-γ-CD system, we detect the sample treated with 0.02-μm filter (see Fig. 1c). The unique peak around 7 nm is reproduced well, exhibiting a slightly larger mass contribution of 0.3206%. Actually, the equilibrium between the monomeric and aggregated forms of γ-CD still exists in the solution, so the aggregates of γ-CD cannot be eliminated even after being treated with 0.02-μm filter. As the intensity of the particle is directly proportional to the cube of its hydrodynamic radius [31], the large size of the aggregates leads to the dominating intensity, and the intensity contribution of the nanotube is still relatively low. The mass contributions of each component show a little difference in the solution of DPB-γ-CD treated with 0.2- and 0.02-μm filters. Gonzalez-Gaitano et al. have traced the intensity and the hydrodynamic radius of the aggregate in the solution of pure γ-CD treated with 0.1-μm filter [31]. The result showed that the aggregated γ-CD was formed and its hydrodynamic radius almost kept unchanged at about 140 nm. They further investigated the aggregation kinetics of pure β-CD solution treated with 0.02-μm filter and the result was similar to that in the pure γ-CD [31]. Consequently, it can be inferred that there exists equilibrium between the monomeric and aggregated forms of CD in the solution from the DLS results of our work and that of Gonzalez-Gaitano et al. [31].

As hydrogen bonding is regarded as an important driving force that benefits the formation of cyclodextrin nanotube [8], the DPB-γ-CD aqueous solution at pH 13.5 is investigated and the DLS result is listed in Table 1. The new peak is now disappeared as shown in Fig. 1d. Since the pK_a value of γ-CD is 12.1 [38], nearly all hydroxyl groups of γ-CD molecule are changed to negative oxygenic ions at pH 13.5, and thus hydrogen bonding between neighboring γ-CD units in the DPB-γ-CD nanotube becomes ineffective leading to the collapse of the nanotubular structure. It is also observed that the mean hydrodynamic radius of the aggregated γ-CD decreases. This can be explained in terms of the fact that when most hydroxyls of γ-CD get ionic at pH 13.5, the repulsion among γ-CD molecules make the self-aggregation difficult. Consequently, the intensity contribution of the aggregated γ-CD is reduced greatly, while the intensity contribution of the monomeric γ-CD is increased substantially. The slight increase in the mean hydrodynamic radius of the monomeric γ-CD seems due to the thicker solvation layer caused by the OH ionization [31].

3.2. Spectral characterization

As shown in Fig. 2, the maximum absorption wavelengths for DPB molecule in pure water, α-, β-, and γ-CD are 336, 336, 341, and 343 nm, respectively. The maximum emission wavelengths (see Fig. 3) are 410, 410, 385, and 385 nm, respectively. The same maximum absorption and emission wavelengths lead us to think that the microenvironment of DPB in water is similar to that in the aqueous solution of α-CD. For the same reason, the microenvironments of DPB are also similar in the aqueous solutions of β- and γ-CD.

It is noted from Fig. 3a that the fluorescence intensity of DPB is increased with increasing α-CD concentration. This suggests that DPB may transfer from water to a less aqueous site and that an inclusion complex might be formed. To estimate the association constant and the stoichiometry of the inclusion complex, the nonlinear regression method [39] with the intensity at a fixed wavelength ($\lambda = 410$ nm for DPB-α-CD, $\lambda = 385$ nm for both DPB-β-CD and DPB-γ-CD) near the maximum emission wavelength has been used. The result as shown in Fig. 3a suggests that only the 1:2 (guest:host) inclusion complex is formed. The estimated K value is $(6.2 \pm 0.6) \times 10^3$ M^{-2} with good correlation coefficient ($r = 0.996$). The interactions between DPB and β-CD are also investigated. The interaction pattern is quite similar to the case of α-CD, i.e., only the 1:2 inclusion complex is formed. The association constant is estimated to be $(1.6 \pm 0.1) \times 10^3$ M^{-2} with $r = 0.996$ (see the inset of Fig. 3b). Comparing these two 1:2 inclusion complexes, one can infer that a smaller cavity of α-CD can result in a stronger interaction and then a larger association constant. For the interaction of DPB with γ-CD, however, none of simple inclusion patterns can yield an agreeable result using nonlinear regression analysis (Fig. 3c).

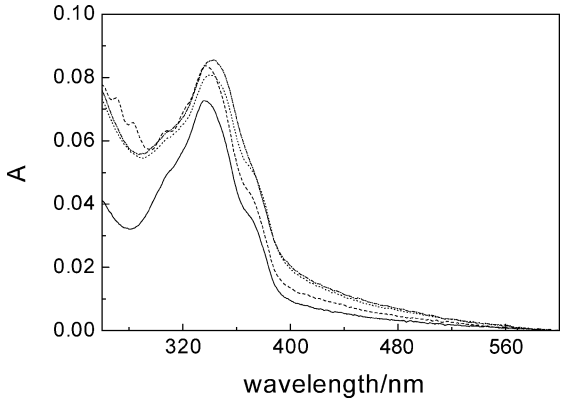

Fig. 2. Absorption spectra of DPB in pure water (solid line), α-CD (dash line), β-CD (dash–dot line), and γ-CD (dot line). [DPB] $= 2 \times 10^{-6}$ M, [CD] = 10 mM.

To our knowledge, the spectral characteristic of DPB is greatly affected by the polarity of microenvironment. Thus, we measured the fluorescence emission of DPB in the mixtures of water and methanol as shown in Fig. 3d. The ratio of the intensity at 385 nm to that at 410 nm (I_{385}/I_{410}) increases with increasing the volume percent of methanol. That is to say, the ratio (I_{385}/I_{410}) increases with increasing the apolarity of solution. Therefore, we think that the different characteristics of the emission of DPB in three CDs may result from its corresponding microenvironments with different polarities. In the case of α-CD that has a small cavity, only part of terminal phenyl group of DPB is included in the cavity and the amine group is still exposed to water. Thus, the polarity of microenvironment detected by DPB in the solution of α-CD is similar to the polarity in pure water or in the methanol–H_2O mixtures at low volume percents of methanol. In the case of β-CD that has a larger cavity, the terminal phenyl group of DPB is deeply included in the hydrophobic cavity and the amine group may reside at the rim of the β-CD cavity. Thus, the polarity of microenvironment of DPB in the solution of β-CD is largely weakened, and the ratio (I_{385}/I_{410}) increases greatly. In the case of γ-CD that has a

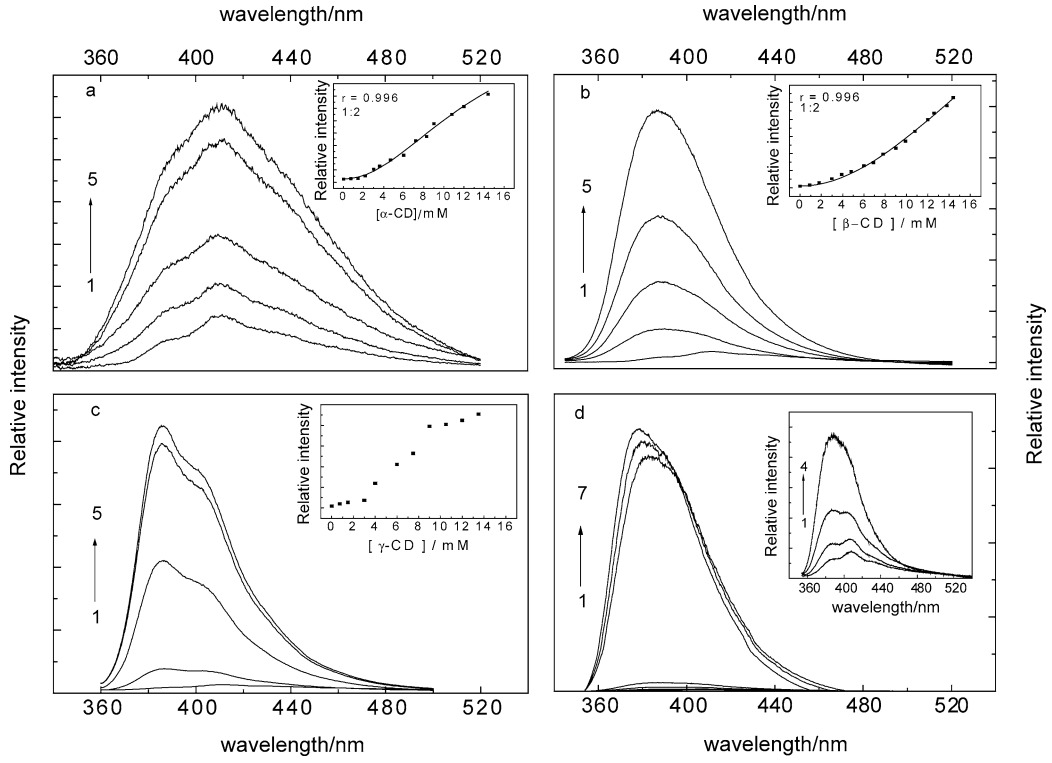

Fig. 3. Fluorescence spectra of DPB (4×10^{-7} M) in the aqueous solutions of α-CD (a), β-CD (b), and γ-CD (c) at various concentrations (from 1 to 5: [CD] = 0, 3, 6, 9, and 12 mM), and in the methanol–H_2O mixture (d) at various volume percents of methanol (from 1 to 7: 0, 20, 30, 40, 60, 80, and 100%).

largest cavity, cyclodextrin nanotube is formed as inferred from the results of DLS. DPB molecule might be partly stacked in the nanotube. Because of the limitation of the space, the location of the phenyl and amine groups of DPB in the case of γ-CD are between those in the cases of α- and β-CD. Thus, the apolarity of microenvironment of DPB in γ-CD is weaker than that in the solution of β-CD but stronger than that in the solution of α-CD.

3.3. Steady-state fluorescence anisotropy

We have measured the steady-state fluorescence anisotropy of DPB in aqueous solutions of α-, β- and γ-CDs. Again, the situation in γ-CD is greatly different from the situations in α- and β-CDs. The large fluorescence anisotropy value of DPB in the aqueous solution of γ-CD is an indication of the formation of nanotube according to Refs. [8,19–23]. The measurement of the steady-state fluorescence anisotropy provides a method to estimate the relative size of the DPB/CD complex according to Perrin–Webber formula [37],

$$r_0/r = 1 + \tau RT/\eta V, \tag{4}$$

where r_0 is the maximum value of anisotropy for a certain probe in a frozen state in which it cannot undergo rotational diffusion. For DPB, the measured value of r_0 is 0.317 in the vitrified solution of glycerol [8], τ is the fluorescence lifetime, η is the viscosity of the medium, T is the absolute temperature and R is the ideal gas constant. When the fluorescence lifetime and viscosity remain constant, an increase in the anisotropy suggests an increase in the size of the complex. Fig. 4a clearly shows a sudden increase in the value of r at relatively low γ-CD concentration, ca. 1–2 mM, and then exhibits a plateau with increasing γ-CD concentration. In contrast, the r values keep small and slightly variable in the aqueous solutions of α- and β-CD. By means of their corresponding r values, the relative size of the DPB-γ-CD nanotube can be estimated with the equation derived from the combination of the Perrin and Einstein equations [8],

$$r_2(r_0 - r_1)/r_1(r_0 - r_2) = V_2/V_1, \tag{5}$$

where r_1 and r_2 are the values of the fluorescence anisotropy measured in two different systems, V_1 and V_2 are the effective volumes of these two systems. In Refs. [8,16,19], it is usually assumed that the viscosity and fluorescence lifetime remain constant in two systems and the number of CD units in a nanotube is then estimated by Eq. (5). To examine the validity of the above assumption, we have measured the viscosity of DPB-CD systems and the corresponding fluorescence lifetimes. To water as a reference, the viscosity ratio (η/η_w) of DPB in water, α-, β-, and γ-CD are 1.02, 1.04, 1.04, and 1.03, respectively. Thus, the viscosity of DPB-CD systems can be regarded as a constant. Then we measured the fluorescence lifetime that is listed in Table 2. We found that fluorescence lifetime of DPB changed with its different microenvironments. Only a short lifetime of 0.48 ns occurred in water, while a longer lifetime was observed in the presence of CDs. Considering a little difference

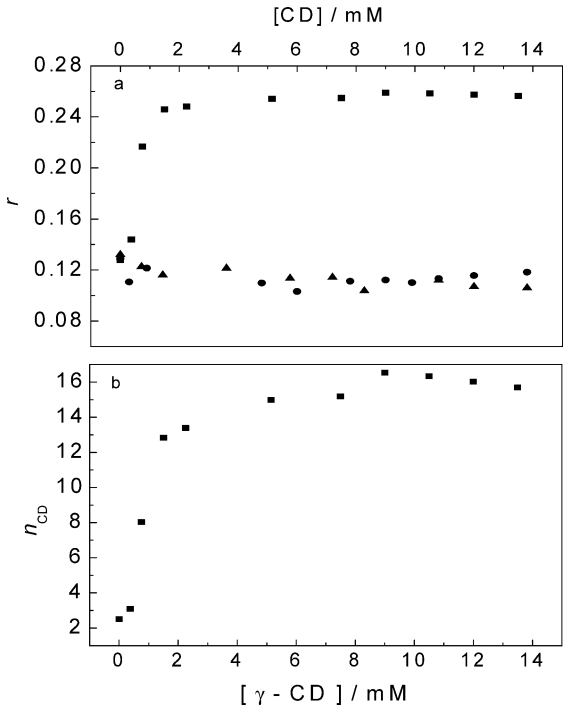

Fig. 4. (a) Fluorescence anisotropy (r) of DPB (4×10^{-7} M) in the aqueous solutions of α-CD (▲), β-CD (●), and γ-CD (■) at various concentrations. (b) The average number of γ-CD units in a nanotube (n_{CD}) at varying γ-CD concentrations.

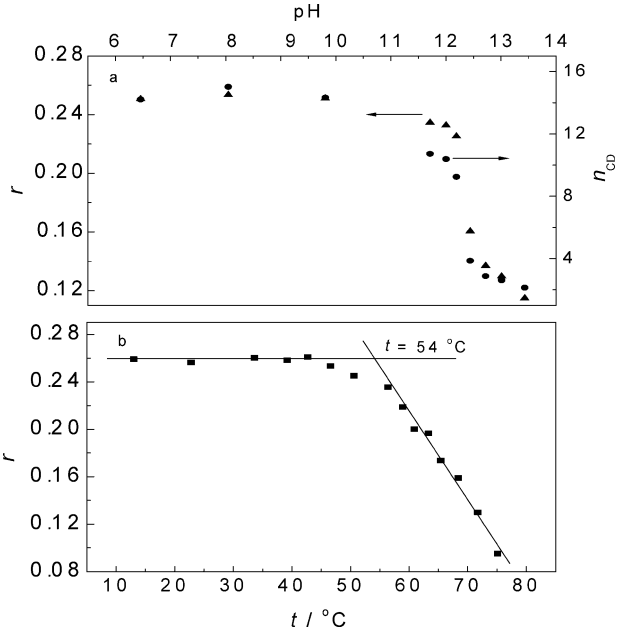

Fig. 5. The steady-state fluorescence anisotropy (r) of DPB (4×10^{-7} M) in the presence of 10 mM γ-CD as a function of pH (a) and temperature (b).

of fluorescence lifetimes of DPB in α- and γ-CD and the comparatively larger difference in the CD cavity size, the error of the estimation of γ-CD units in a nanotube by Eq. (5) would be about 20% based on DPB-α-CD 1:2 inclusion complex. On the contrary, due to the similar viscosity and fluorescence lifetime values of DPB in β- and γ-CD systems as well as small difference in the CD cavity size, the value of $2 \times (V_2/V_1)$ ob-

Table 2
Fluorescence lifetimes of DPB in water, aqueous solutions of α-, β-, and γ-CD. [DPB] = 2×10^{-6} M, [CD] = 10 mM

Medium	τ_1 (ns)	B_1	τ_2 (ns)	B_2[a]	χ^2
Water	0.48 ± 0.01	1.00	–	–	1.12
α-CD	0.54 ± 0.02	0.79	2.87 ± 0.07	0.21	1.32
β-CD	0.46 ± 0.01	0.88	3.60 ± 0.09	0.12	1.07
γ-CD	0.47 ± 0.01	0.87	3.45 ± 0.09	0.13	1.21

[a] B_i is a preexponential factor representing the fractional contribution to the time-resolved decay of the component with a lifetime τ_i, $I(t) = \sum_i B_i e^{-t/\tau_i}$.

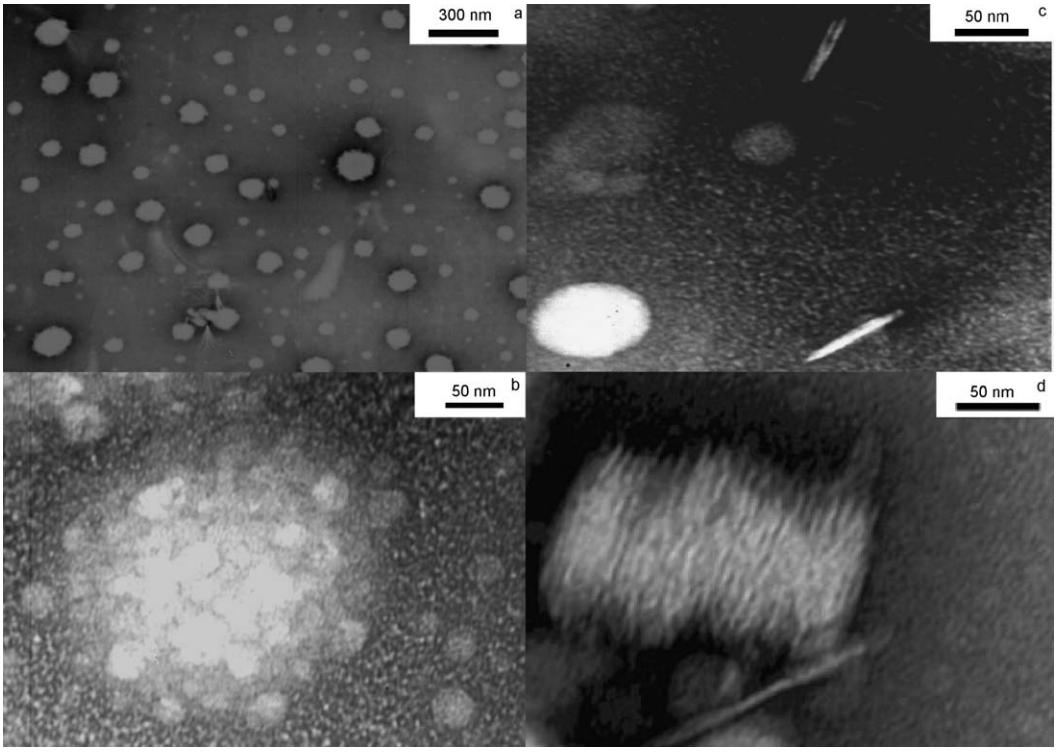

Fig. 6. TEM images of aggregated γ-CD ((a) and (b)), DPB-γ-CD nanotube (c), and secondary aggregation of DPB-γ-CD nanotubes (d). For (a) and (b), [γ-CD] = 10 mM; for (c) and (d), [DPB] = 4×10^{-7} M, [γ-CD] = 10 mM.

tained from Eq. (5) is approximate to the average number of γ-CD units in a nanotube. From Fig. 4a, the r_1 value is 0.112 in the 1:2 DPB-β-CD inclusion complex. In this case, the maximum number of γ-CD units in a nanotube was estimated to be 16, as shown in Fig. 4b. These results agree well with the DLS analysis results, that is, the size of cyclodextrin nanotube is much larger than that of the inclusion complex.

To confirm the contribution of hydrogen bonding to the nanotube formation, the pH influence on the DPB-γ-CD aqueous solution is studied again with fluorescence anisotropy. As shown in Fig. 5a, the r value remains unchanged at low pH values, but is decreased abruptly when the pH value rises above 12.00. This result is in accordance with the report in Refs. [8,19,23] and strongly supports the conclusion obtained by DLS.

To discuss the thermostabilization of this cyclodextrin nanotube, we measured the fluorescence anisotropy of DPB as a function of temperature. As presented in Fig. 5b, the r value remains almost invariable until the temperature is increased beyond 50 °C. The transition point is estimated to be around 54 °C. This means that the DPB-γ-CD nanotube could exist stably at a relatively high temperature compared to some other cyclodextrin nanotubes reported earlier [23]. It may have some potential application in the field of temperature controlling molecular wires [40–43]. We believe this fact can help understanding the mechanism of the formation of cyclodextrin nanotube.

3.4. TEM images

Spherical aggregates of γ-CD molecules with diameters of 50–150 nm were observed using TEM as shown in Fig. 6a. The monomeric form of γ-CD was not detected in the field of vision. Interestingly, the spherical aggregates of γ-CD seem to aggregate further to a loose structure (Fig. 6b). Fig. 6c shows the single DPB-γ-CD nanotube, while Fig. 6d shows the secondary aggregation of nanotubes in the same solution. High-resolution TEM is further used to observe the topology of DPB-γ-CD and the nanotubular structure is shown in Fig. 7. In crystal structure, cyclodextrin itself and some cyclodextrin inclusion complexes are known to form cage- and channel-type structures [44–47]. However, since Li and his co-workers

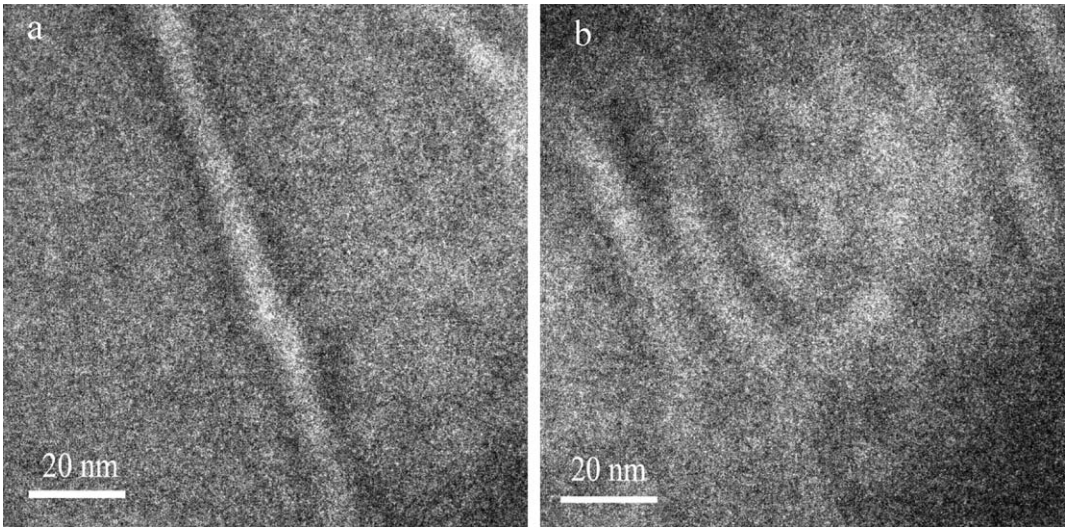

Fig. 7. High-resolution TEM images of DPB-γ-CD nanotube (a) and secondary aggregation of DPB-γ-CD nanotubes (b). [DPB] $= 4 \times 10^{-7}$ M, [γ-CD] $= 10$ mM.

observed the DPH-β-CD nanotube by STM in 1994 [7], the detailed structural characteristic of this kind of cyclodextrin nanotube has been rarely reported [13–15,48]. Very recently, Liu et al. reported that a linear structure was obtained from β-CD/4-hydroxyazobenzene complex by the intra- and inter-dimer hydrogen bonding as well as the intradimer π–π interactions, while a wave-type structure was obtained when 4-aminoazobenzene acted as the guest molecule [15]. Based on Liu's work, we propose here that the single DPB-γ-CD nanotube is likely to adopt the wave-type structure other than the linear structure due to the none-linear molecular structure of DPB itself (see Scheme 1). To the best of our knowledge, the secondary aggregation of nanotubes of DPB-γ-CD in Figs. 6d and 7b has never been observed before. Ravoo et al. observed elongated tape-like structures formed by the self-assembly of a 'Janus' cyclodextrin [49]. It was proposed that the elongated tapes resulted from an efficient hydrogen bonding network among the 'Janus' cyclodextrin molecules. Moreover, in the process of an amphiphilic hyperbranched copolymer aggregated to a macroscopic multiwalled tube, the formation of hydrogen bonding in both core and arm lamellae also facilitated the self-assembly greatly [50]. Thus, we consider that, here, it is the hydrogen bonding between each DPB-γ-CD nanotube which further drives the molecular self-assembly process and strengthens the secondary aggregation of cyclodextrin nanotubes.

4. Conclusions

Dynamic light scattering measurement as an effective method suggested different interaction patterns of DPB with α-, β-, and γ-CDs. With the combination of steady-state fluorescence and fluorescence anisotropy experiments, we found that 1:2 (guest:host) inclusion complex was formed between DPB and α- or β-CD, and nanotube was formed between DPB and γ-CD. The pH effect studies with both DLS and fluorescence anisotropy strongly suggested the significant contribution of hydrogen bonding to the formation of cyclodextrin nanotube. The temperature study indicated that this DPB-γ-CD nanotube could exist stably at a relatively high temperature and the transition point for the nanotube collapse was estimated to be around 54 °C. TEM images clearly showed the aggregation of γ-CD and DPB-γ-CD nanotube which supported the results of DLS and fluorescence anisotropy.

Acknowledgments

This work was supported by the National Natural Science Foundation of China (Grants 90206020, 29901001) and Doctoral Program Foundation of Education Ministry of China (Grant 20010001003).

References

[1] (a) H.J. Schneider, F. Hacket, V. Rudiger, H. Ikeda, Chem. Rev. 98 (1998) 1755;
(b) R. Breslow, S.D. Dong, Chem. Rev. 98 (1998) 1997.
[2] E. Engeldinger, D. Armspach, D. Matt, Chem. Rev. 103 (2003) 4147.
[3] (a) Y. Chen, T. Xu, X. Shen, H. Gao, J. Photochem. Photobiol. A Chem. 173 (2005) 42;
(b) X. Shen, M. Belletête, G. Durocher, Chem. Phys. Lett. 301 (1999) 193;
(c) H. Asanuma, M. Kakazu, M. Shibata, T. Hishiya, M. Komiyama, Chem. Commun. 20 (1997) 1971.
[4] (a) G. Wenz, B. Keller, Angew. Chem. Int. Ed. Eng. 31 (1992) 197;
(b) E. Alami, S. Abrahmsén-Alami, J. Eastoe, I. Grillo, R.K. Heenan, J. Colloid Interface Sci. 255 (2002) 403.
[5] A. Harada, J. Li, M. Kamachi, Nature 356 (1992) 325.
[6] A. Harada, J. Li, M. Kamachi, Nature 364 (1993) 516.
[7] G. Li, L.B. McGown, Science 264 (1994) 249.
[8] G. Pistolis, A. Malliaris, J. Phys. Chem. 100 (1996) 15562.
[9] G. Pistolis, A. Malliaris, J. Phys. Chem. B 102 (1998) 1095.
[10] A.A. Rezik, D. David, J. Phys. Chem. 92 (1988) 1052.
[11] R.A. Agbaria, D. Gill, J. Photochem. Photobiol. A Chem. 78 (1994) 161.
[12] A.A. Kimberly, D.M. Tracy, A.A. Rezik, M.W. Isiah, J. Photochem. Photobiol. A Chem. 91 (1995) 205.
[13] Y. Liu, C.-C. You, H.-Y. Zhang, S.-Z. Kang, C.-F. Zhu, C. Wang, Nano Lett. 1 (2001) 613.
[14] Y. Liu, H. Wang, P. Liang, H.-Y. Zhang, Angew. Chem. Int. Ed. 43 (2004) 2690.
[15] Y. Liu, Y.-L. Zhao, Y. Chen, D.-S. Guo, Org. Biomol. Chem. 3 (2005) 584.
[16] (a) X. Wen, M. Guo, Z. Liu, F. Tan, Chem. Lett. 33 (2004) 894;
(b) I. Topchieva, K. Karezin, J. Colloid Interface Sci. 213 (1999) 29.

[17] S. Makedonopoulou, I.M. Mavridis, K. Yannakopoulou, J. Papaioannou, Chem. Commun. 19 (1998) 2133.
[18] Y. Liu, Z. Fan, H.-Y. Zhang, Y.-W. Yang, F. Ding, S.-X. Liu, X. Wu, T. Wada, Y. Inoue, J. Org. Chem. 68 (2003) 8345.
[19] C. Zhang, X. Shen, H. Gao, Chem. Phys. Lett. 363 (2002) 515.
[20] C. Zhang, X. Shen, H. Gao, Spectrosc. Spect. Anal. 23 (2003) 217.
[21] K. Xia, T. Hou, X. Xu, X. Shen, Acta Physico-Chimi. Sinica 20 (2004) 5.
[22] (a) C. Zhang, Ph.D. thesis, Peking University, Beijing, 2002;
(b) K. Xia, M.Sc. thesis, Peking University, Beijing, 2004;
(c) X. Chen, M.Sc. thesis, Peking University, Beijing, 2005.
[23] A. Wu, X. Shen, H. Gao, Int. J. Nanosci. (2005), in press.
[24] (a) P. Robert, Dynamic Light Scattering: Applications of Photon Correlation Spectroscopy, Plenum, New York, 1985;
(b) W. Brown, Light Scattering, Oxford Univ. Press, Oxford, UK, 1996.
[25] (a) M. Almgren, J.C. Gimel, K. Wang, G. Karlsson, K. Edward, W. Brown, K. Mortensen, J. Colloid Interface Sci. 202 (1998) 222;
(b) A. Sandier, W. Brown, H. Mays, C. Amiel, Langmuir 16 (2000) 1634;
(c) A. Valstar, M. Almgren, W. Brown, M. Vasilescu, Langmuir 16 (2000) 922;
(d) L. Bastardo, P. Claesson, W. Brown, Langmuir 18 (2002) 3848;
(e) E. Feitosa, W. Brown, K. Wang, P.C.A. Barreleiro, Macromolecules 35 (2002) 201;
(f) W. Brown, P. Stepanek, J. Polym. Sci. Pol. Phys. 35 (1997) 1013;
(g) H. Kunieda, M. Kaneko, M.A. Lopez-Quintela, M. Tsukahara, Langmuir 20 (2004) 2164;
(h) C. Rodriguez-Abreu, M. Garcia-Roman, H. Kunieda, Langmuir 20 (2004) 5235.
[26] G. Gaitano, W. Brown, J. Phys. Chem. B 101 (1997) 710.
[27] O. Häusler, C.C. Müller-Goymann, Starch 45 (1993) 183.
[28] N. Azaroual-Bellanger, B. Perly, Magn. Reson. Chem. 32 (1994) 8.
[29] A.W. Coleman, I. Nicolis, N. Keller, J.P. Dalbiez, J. Incl. Phenom. Mol. Recognit. Chem. 13 (1992) 139.
[30] L. Moine, C. Amiel, W. Brown, P. Guerin, Polym. Int. 50 (2001) 663.
[31] G. Gonzalez-Gaitano, P. Rodriguez, J.R. Isasi, M. Fuentes, G. Tardajos, M. Sanchez, J. Incl. Phenom. Macrocycl. Chem. 44 (2002) 101.
[32] A. Mazzaglia, N. Angelini, D. Lombardo, N. Micali, S. Patane, V. Villari, L.M. Scolaro, J. Phys. Chem. B 109 (2005) 7258.
[33] J.J. Niu, J.Y. Lee, A. Neudeck, L. Dunsch, Synth. Met. 99 (1999) 133.
[34] A. Balionyte, S. Grigalevicius, V. Jankauskas, G. Garsva, J.V. Grazulevicius, J. Photochem. Photobiol. A Chem. 162 (2004) 249.
[35] B. Lu, H.J. Zhang, Y. Li, S.N. Bao, P. He, T.L. Hao, Phys. Rev. B 68 (2003) 125,410.
[36] F. Han, X. He, J. Huang, Z. Li, Y. Wang, H. Fu, J. Phys. Chem. B 108 (2004) 5256.
[37] J.R. Lakowicz, Principles of Fluorescence Spectroscopy, Plenum, New York, 1983.
[38] R.I. Gelb, L.M. Schwartz, J.J. Bradshaw, D.A. Laufer, Bioorg. Chem. 9 (1980) 299.
[39] X. Shen, M. Belletête, G. Durocher, Chem. Phys. Lett. 298 (1998) 201.
[40] K.A. Agnew, T.D. McCarley, R.A. Agbria, I.M. Warner, J. Photochem. Photobiol. A Chem. 78 (1994) 85.
[41] W.B. Davis, M.A. Ratner, M.R. Wasielewski, J. Am. Chem. Soc. 123 (2001) 7877.
[42] J. Lehmann, G.L. Ingold, P. Hanggi, Chem. Phys. 281 (2002) 199.
[43] N. Kimizuka, N. Oda, T. Kunitake, Inorg. Chem. 39 (2000) 2684.
[44] K. Harata, Bull. Chem. Soc. Jpn. 48 (1974) 2049.
[45] K. Harata, Chem. Rev. 98 (1998) 1083.
[46] S. Yasuda, K. Miyake, J. Sumaoka, M. Komiyama, H. Shigekawa, Jpn. J. Appl. Phys. 38 (1999) 3888.
[47] S.S. Braga, I.S. Goncalves, E. Herdtweck, J.J.C. Teixeira-Dias, New J. Chem. 27 (2003) 597.
[48] K. Miyake, S. Yasuda, A. Harada, J. Sumaoka, M. Komiyama, H. Shigekawa, J. Am. Chem. Soc. 125 (2003) 5080.
[49] B.J. Ravoo, R. Darcy, A. Mazzaglia, D. Nolan, K. Gaffney, Chem. Commun. 9 (2001) 827.
[50] D. Yan, Y. Zhou, J. Hou, Science 303 (2004) 65.